Segmented Poly(tetramethylene oxide) Zwitterionomers and Their Homologous Ionenes. 2. Phase Separation through DSC and Solid State1H-NMR Spectroscopy

ARTICLE *in* MACROMOLECULES · JANUARY 1997

Impact Factor: 5.8 · DOI: 10.1021/ma960643s

4 AUTHORS, INCLUDING:

Bruno Grassl
Université de Pau et des Pays de l'Adour
74 PUBLICATIONS **873** CITATIONS

Segmented Poly(tetramethylene oxide) Zwitterionomers and Their Homologous Ionenes. 2. Phase Separation through DSC and Solid State ^{1}H-NMR Spectroscopy

Bruno Grassl, Bernard Meurer, Monique Scheer, and Jean Claude Galin*

Institut Charles Sadron, CNRS-ULP, 6 rue Boussingault, 67083 Strasbourg Cedex, France

Received May 1, 1996; Revised Manuscript Received September 24, 1996[⊗]

ABSTRACT: Phase separation has been quantitatively analyzed through DSC and solid state ^{1}H-NMR spectroscopy (line shape and $T_1\rho$ analysis) on a series of segmented PTMO zwitterionomers carrying dipolar functions of the ammoniopropanesulfonate or ethoxydicyanoethenolate type and of their analogous ionenes. All the amorphous copolymers (M_n^0(PTMO segment) < 3×10^3) display a typical biphasic structure characterized by a strongly predominant soft matrix of pure PTMO ($T_g^S = -77$ °C) and polar hard domains ($T_g^H = -5$ to 40 °C) where all the polar junctions are concentrated and where every polar unit locks and rigidifies about the two or three vicinal PTMO monomeric units. The thermal stability of the polar aggregates which persist at temperatures much higher than the glass transition T_g^H depends on their chemical structure: for promoting high cohesion, zwitterions are much more efficient than ion pairs (zwitterionomers versus ionenes) and the ammoniopropanesulfonate function is more efficient than the ethoxydicyanoethenolate one in spite of similar dipole moments (∼25 D). Semicrystalline copolymers (M_n^0(PTMO segment) > 3×10^3) still show phase separation in their amorphous state in the higher temperature range above their melting points ($T_m \sim 10-25$ °C). The typical biphasic morphologies of all these copolymers may be readily interpreted within the multiplet−cluster concept revisited by Eisenberg, and the rigidification of the PTMO units immediately surrounding the polar multiplets is unambiguously evidenced in solid state NMR spectroscopy. The specific segmented chain topology results, however, in an earlier (lower polar unit contents) and far better phase separation than in similar statistical copolymers.

Introduction

Previous studies in our laboratory have clearly shown that statistical amorphous zwitterionomers combining weakly polar *n*-butyl acrylate A units and low to moderate amounts (molar fraction ∼ 0.04−0.35) of highly dipolar zwitterionic B units of the ammoniopropanesulfonate[1−4] or (ammonioethoxy)dicyanoethenolate[5] type (functional side groups $N^+(CH_2)_3SO_3^-$, μ = 24 D, or $N^+(CH_2)_2OCOC^-(CN)_2$, μ = 25.9 D, respectively) show a very typical two-phase morphology: it is essentially characterized by the dispersion of zwitterion-rich and "hard" microdomains in a fairly pure A "soft" matrix, without any long range order. The close analogy with the well-known ionomers[6−9] is quite evident: the strong dipolar interactions between the zwitterionic units within the very mobile and only weakly polar matrix are the driving force of the observed microphase separation. These complex heterogeneous structures may be readily analyzed within the "multiplet−cluster" concepts recently revisited by Eisenberg et al.[10] or within the elegant framework of phase separation in multiblock copolymers considered in the so-called "superstrong segregation regime" (very high Flory χ(A−B) interaction parameter, which is precisely the case of ionomers and zwitterionomers) and extrapolated to the limiting case of only one polar B unit per polar block.[11] On the other hand, we described in the first paper of this series the synthesis and the molecular characterization of a series of homologous segmented zwitterionomers and ionenes based on poly(tetramethylene oxide) (PTMO) corresponding to the general formula:[12]

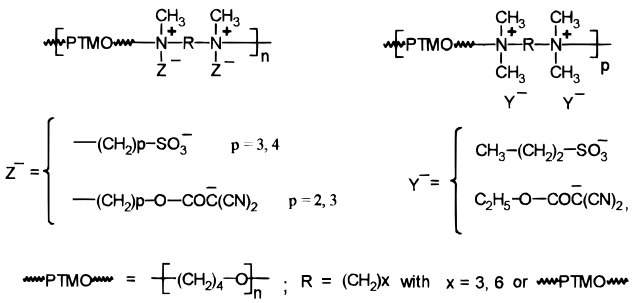

In these model copolymers, the chain topology is characterized by the regular alternation of weakly polar PTMO segments of well-controlled molecular weight and polydispersity ($M_n^0 \sim (1.7-8.0) \times 10^3$, $M_w^0/M_n^0 \leq 1.15$) and of strongly polar zwitterionic or ionic short junctions of functionality $f = 1$ (R = PTMO segment) or $f = 2$ (R = $(CH_2)_x$). It is thus quite different from that of the previously discussed statistical zwitterionomers and ionomers, and it may likely result in some specific structural features. The purpose of the present work is thus to analyze quantitatively the microphase separation in this series of homologous PTMO-segmented zwitterionomers and ionenes as a function of chain structure with special emphasis on the following points:

- influence of the density of the polar junctions along the chain
- influence of the chemical structure of the polar units and, more specifically, comparison between homologous zwitterions and ion pairs characterized by identical

[⊗] Abstract published in *Advance ACS Abstracts*, December 15, 1996.

S0024-9297(96)00643-2 CCC: $14.00

Table 1. DSC Analysis (Standard Thermal Cycle) of the Segmented Polymers[a]

copolymer	W_B	T_g^S (°C)	ΔC_p^S (J·g^{-1}·K^{-1})	T_c (°C)	ΔH_c (J.g^{-1})	T_m (°C)	ΔH_m (J.g^{-1})	T_g^H (°C)	ΔC_p^H (J·g^{-1}·K^{-1})
Z20-E3-6	0.184	−77	0.43					15	0.12
Z17-E2-3	0.179	−76	0.48					24	0.12
Z20-S4-6	0.174	−78	0.48					21	0.13
Z17-S3−3	0.167	−77	0.52					16	0.09
Z20-S3-6	0.164	−77	0.47					38	0.17
Z22-E2-6	0.161	−77	0.48					25	0.17
Z36-E2-6	0.103	−78	0.45	−41	−16.4	7	16.9		
Z37-S3-6	0.096	−78	0.28	−52	−7.2	15	32.8		
Z52-E2-6	0.074	−78	0.23	−57	−6.6	19	40.5		
Z52-S3-6	0.070	−75	0.17			17	39.3		
Z67-E2-6	0.059	−77	0.19			25	49.2		
Z67-S3-6	0.055	−76	0.2			22	44.5		
Z19-E2	0.080	−78	0.60			17	0.8		
Z19-S3	0.073	−79	0.62	−3	−3.8	20	5		
I19-E-6	0.191	−75	0.41					6	0.09
I19-S-6	0.182	−77	0.48					−4	0.10

[a] All the ΔCp values are the primary apparent values normalized to 1 g of copolymer. $Tg = -77 \pm 1$ °C and $Tm \sim 28-30$ °C for PTMO α,ω-diol ($Mn^0 \sim 2.2-6.7 \times 10^3$).

structures of the charged sites (zwitterionomers versus ionenes) and comparison with literature data related to similar PTMO segmented ionenes[13−15]

•influence of the chain topology by comparison with literature data on zwitterionomers bearing the same functional groups: segmented versus statistical copolymers (the very important question of the potential development of long range order (spatial organization of the polar domains) favored by the specific segmented topology of the chain will be, however, addressed in a forthcoming paper)

The analysis of chain dynamics through two different methods, differential scanning calorimetry (DSC) and solid state broad line nuclear magnetic resonance spectroscopy (line shape and $T_1\rho$ analysis), will be systematically used for the identification of the coexisting phases in the bulk materials and for a quantitative structural description in terms of internal composition and relative importance of the polar domains and of the nonpolar matrix. The sample identification systematically used throughout the following text allows us to identify successively zwitterionomers (Z) or ionenes (I), the molecular weight of the PTMO block (M_n^0/100), zwitterions or ion pairs of the alkanesulfonate (S*p*) or alkoxydicyanoethenolate (E*p*) type with *p* methylene groups in the intercharge arm for zwitterionic structures, and finally, the number of methylene groups *x* in the short diamino segment:

$$\text{Z or I } M_n^0(\text{PTMO})/100 - \text{Sp or Ep} - x$$

Thus, sample Z22-E3-6 is a zwitterionomer carrying PTMO segments of number average molecular weight 2.2×10^3, functionalized with an (ammoniopropoxy)-dicyanoethenolate structure separated by a short segment of six methylene groups. Sample I22-E-6 is the homologous ionene, where the figure *p* has been obviously deleted. Z19-S3 is a zwitterionomer carrying monofunctional ammoniopropanesulfonate junctions between PTMO segments of $M_n^0 = 1.9 \times 10^3$.

Experimental Section

Materials. The synthesis and molecular characterization of the various PTMO zwitterionomers and ionenes were described previously.[12] The weight average degrees of polycondensation in the segmented chains are never lower than 15, and the overall polydispersity indexes of the copolymers are about 2. The synthesis of the polymeric models of the zwitterionic structures S3 and E2, PZ-S3-6 and PZ-E2-6 is detailed elsewhere[16] (see Results and Discussion for the chemical formula).

Differential Scanning Calorimetry (DSC). DSC measurements were performed on Perkin-Elmer DSC 7 and DSC 4 apparatus (low and high temperature ranges) interfaced with a computer data station, after previous calibration with *n*-decane, gallium, and indium, $T_m = -29.7$, 29.8, 156.6 °C, respectively. About 10−15 mg of the previously dried samples were weighted with an accuracy of ±0.03 mg in stainless steel pans and they were further dried at 60 °C under vacuum (<0.1 Torr) for at least 4 days, before sealing the pans under argon at 60 °C directly in the oven fitted with a vacuum−argon flow system. Residual moisture should be thoroughly eliminated since it may result in selective plasticization of the hard domains and redistribution of the zwitterionic units in less numerous multiplets of increased aggregation number, as previously shown in *n*-butyl acrylate statistical zwitterionomers.[4] The crystallization and melting temperatures, T_c and T_m, were measured at the maximum of the exothermic and endothermic peaks, respectively, and the glass transition temperature was determined at the midpoint of the baseline shift ($\Delta C_p/2$). The transition width was estimated by $\Delta T = T_2 - T_1$, where T_1 and T_2 are the intersections of the extrapolated glassy and liquid baselines with the tangent to the thermogram inflection point. Thermal cycles were systematically repeated until reproducible scans were obtained. In the standard heating−cooling sequences adopted for all the segmented zwitterionomers and ionenes and for reference PTMO, a temperature range from −130 to +130 °C was alternatively scanned with cooling and heating rates of 40 and 20 K·min^{-1}, respectively. The reproducibility obtained generally after the second cycle was about ±2 deg on the crystallization, melting, and glass transition temperatures T_c, T_m, and T_g, about ±0.02 J·g^{-1}·K^{-1} for the heat capacity increments ΔC_p at T_g, and about ±0.5 J·g^{-1} for the crystallization or melting enthalpies ΔH_c and ΔH_m.

Solid State ^{1}H-NMR Spectroscopy. The copolymers were dried as previously described for DSC, directly in the NMR tubes which were finally flushed with argon before any experiment. Measurements were performed on a Bruker SXP spectrometer operating at 60 and 90 MHz. For ^{1}H wide-line analysis signals were digitized with 12 bits (accuracy 1/2000) at a fastest sampling rate of 5 MHz (Lecroy 6818). In the AD converter, the memory is filled at a lower sampling rate to obtain simultaneously an accurate baseline and the slowly decaying component (sampling between 100 kHz and 1 MHz). A signal/noise ratio of 500 by digital averaging was typical for adjusting sums of exponentials (≤2 components) by iterative least squares nonlinear fits. Gaussian functions were adjusted to the fast decaying part of the FID, allowing extrapolation through the 5 μs dead time to the origin of the FID (taken at the middle of the 90° of pulse).[17] Deconvolution into Gaussian components was performed only where the ratio of their characteristic spin−spin relaxation times T_2 was

higher than 3. The ^{1}H rotating frame spin−lattice relaxation time, $T_1\rho$, was measured by the sequence 90-spin lock-observation.[17] To analyze the wide spectra of decay constants, at least 50 locking durations were recorded on each decay. The spin locking field was adjusted to 50 kHz.

Results and Discussion

For simplification, the TMO units and the zwitterionic or ionic junctions will be identified as the A and B components of the segmented chain and the composition of the copolymer or of its various phases will be expressed in terms of their molar, weight, or hydrogen fraction (^{1}H-NMR) F_i, W_i, and Φ_i, respectively (i = A or B). Structural data derived from the DSC and solid state NMR analysis will be discussed successively.

Structural Analysis through DSC Measurements. Segregation of Polar Domains in the Amorphous or Semicrystalline Systems. The experimental results and the three representative thermograms given in Table 1 and in Figure 1 clearly show three major points.

(a) Whatever the composition, all the copolymers display the same narrow glass transition at low temperature, T_g^S, identical to that of the pure reference PTMO homopolymer:

$$T_g^S = T_g^{An} = -77 \pm 2\ °C, \qquad \Delta T = 10 \pm 2\ °C$$

(b) For the higher polar junction contents, $0.16 \leq W_B \leq 0.19$ ($M_n^0 \leq 2.2 \times 10^3$, $f = 2$), the zwitterionomers and ionenes are amorphous materials (lack of any melting endotherm) which display a second broader glass transition ($\Delta T = 25-35$ °C) in a higher temperature range, T_g^H. Its position depends on the chemical structure of the polar units, and it occurs at temperatures higher for zwitterionomers ($T_g^H = 15-38$ °C) than for ionenes (−4 to +6 °C).

These two features confirm without any ambiguity the biphasic morphology of these amorphous copolymers characterized by the coexistence of a soft phase of pure PTMO (T_g^S) and of a hard phase containing all the polar junctions and a low fraction of the TMO units (T_g^H). Quantitative analysis of this two-phase structure will be discussed further in the text.

(c) For the lower polar junction contents, $0.06 \leq W_B \leq 0.10$ ($M_n^0 = 1.1 \times 10^3$ with $f = 1$, $M_n^0 > 2.2 \times 10^3$ with $f = 2$), only the transitions of the soft PTMO phase are clearly identified: glass transition of the amorphous fraction at -77 ± 2 °C, partial recrystallization between −60 and −20 °C and, finally, melting of the crystalline fraction between −20 and +40 °C. The melting endotherms are, however, strong enough and cover a broad enough temperature range in order to mask eventually a second glass transition: compare, for instance, thermograms 1a and 1b in the temperature range around T_g^H and T_m. Moreover, on the thermogram 1c, the weak ΔC_p observed when crossing the melting endotherm may be related more likely to a glass transition occurring within the same temperature range and involving a very small fraction of the material rather than to an erratic fluctuation of the baseline during the temperature scan.

A series of thermal treatments were thus applied to zwitterionomers Z52-S3-6 and Z67-S3-6, chosen as representative semicrystalline samples, in order to reveal the possible high-temperature glass transition of the dipolar domains. After melting at 90 °C, the samples were quenched and kept for 5 min at a given temperature T_i, the initial temperature of the DSC scan; the temperature was then increased up to 90 °C at a heating rate of 10 K·min^{-1}. Three behaviors may be readily differentiated according to the T_i value:

(i) for any $T_i < -10$ °C, sample crystallization under cooling can never be avoided, even for very fast quenching rates (200 K·min^{-1}, or inserting for 5 min the DSC pan in an aluminum block precooled in liquid nitrogen, before transfer to the calorimeter previously cooled at −130 °C). It was not thus possible to observe successively the two glass transitions T_g^S and T_g^H during the same DSC scan.

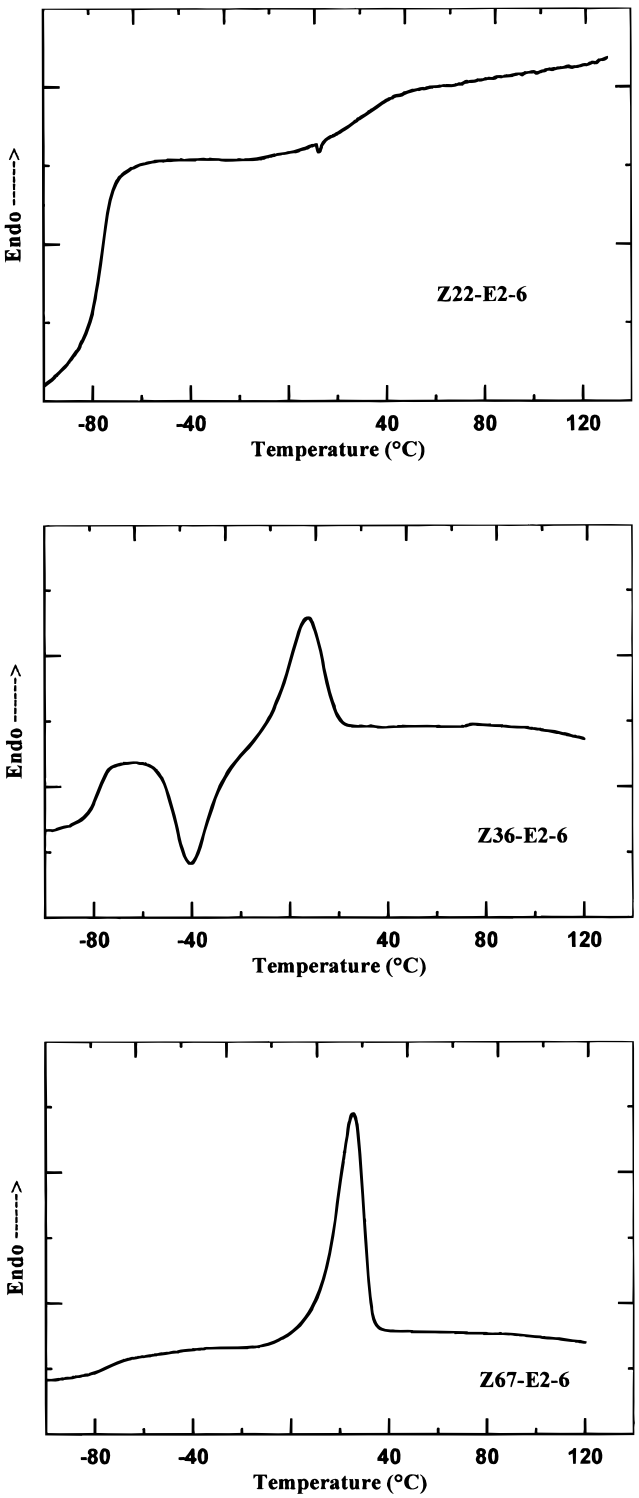

Figure 1. DSC thermograms of three representative zwitterionomers.

(ii) For $T_i = 0$ °C, however, and even for much slower quenching rates (40 K·min^{-1}), the thermograms lack any melting endotherm and do show a rather broad glass transition which is quite reproducible on successive scans:

Z52-S3-6 $T_g^H = 44$ °C $\Delta T = 33$ °C
$\Delta C_p^H = 0.10$ J·g^{-1}·K^{-1}

Z67-S3-6 $T_g^H = 45$ °C $\Delta T = 40$ °C
$\Delta C_p^H = 0.08$ J·g^{-1}·K^{-1}

(iii) Finally, for $T_i = 25$ °C, crystallization can be detected only after an annealing for at least 1 week. Very slow crystallization kinetics at room temperature have already been noticed on some segmented PTMO ionenes.[13]

Thus, DSC measurements performed according to procedure ii confirm the biphasic morphology of these two zwitterionomers considered in their metastable amorphous state: as expected, there is no discontinuity in the copolymer structure with respect to their dipolar content W_B. For the homologous zwitterionomers of the dicyanoethenolate type Z52-E2-6 and Z67-E2-6, the suitable quenching temperature T_i should be high enough to avoid any crystallization but lower than the potential T_g^H (by at least 30 deg) in order to allow a reliable identification of the glass transition of the polar domains: such a T_i temperature could not be found. This behavior merely arises from the T_g^H decrease when going from sulfonate to dicyanoethenolate structures for zwitterionomers of otherwise similar PTMO segment length and functionality: see Table 1 and further discussion.

Crystallization of the Zwitterionomers. Its detailed study is beyond the scope of the present work, but the DSC experimental data obtained in the standard thermal treatment of the various copolymers (see Experimental Section) may be briefly analyzed in terms of variations of the melting temperature T_m and of the crystallinity degree X_C with composition W_B:

$$X_C = \frac{\Delta H_m}{(1 - W_B)\Delta H_m^0} \quad (1)$$

where ΔH_m is the apparent melting enthalpy normalized to 1 g of copolymer.

The literature values of the melting enthalpy of PTMO, ΔH_m^0, are broadly scattered between 152 and 200 J·g^{-1} and calculations were performed using the value of 167 J·g^{-1} derived from a study of PTMO crystallization by DSC and solid state broad line NMR spectroscopy.[18] The crystallinity degree X_C and the melting temperature T_m are quasi linear decreasing functions of the zwitterionic content, as shown in Figure 2. For a bifunctional dipolar junction, extrapolation leads to a minimum value of the PTMO block molecular weight M_n^0 necessary for significant crystallization, $M_n^0 \sim 3 \times 10^3$, whatever the structure of the zwitterion. This estimation is in good agreement with the amorphous character of the various bifunctional zwitterionomers Z17, Z20, and Z22 and still remains self-consistent with the very low crystallization degrees measured on the zwitterionomers Z19-E2 and Z19-S3 ($X_C < 0.05$) where the influence of the shorter PTMO segment length is balanced by the presence of a monofuntional

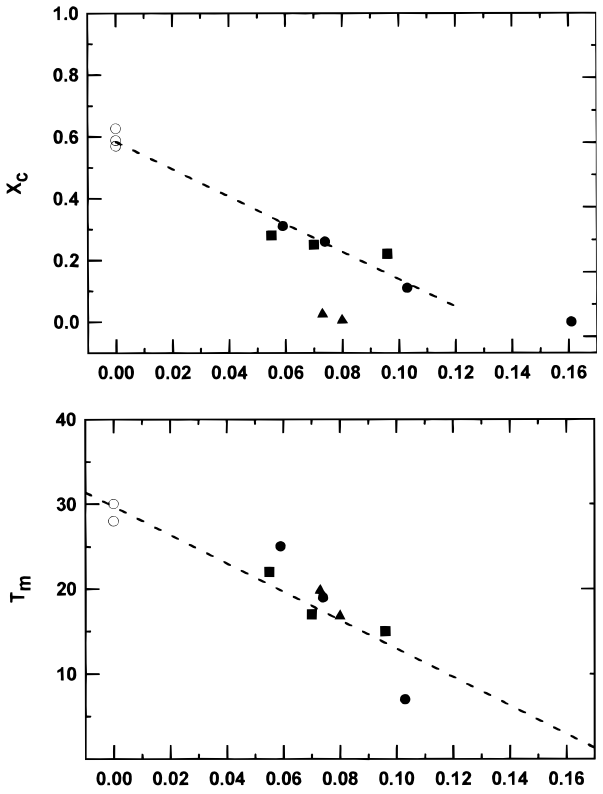

Figure 2. Variations of the crystallinity degree X_c and of the melting temperature T_m with composition W_B for various series of zwitterionomers (standard thermal cycle): E2-6 (●); S3-6 (■); Z19-E2 and S3 (▲); PTMO α,ω-diol ($M_n^0 \sim (2.2-6.7) \times 10^3$) (○).

junction. The T_m and X_C values reported in Figure 2 are obviously strictly related to the well-defined thermal history of the copolymers (standard cycle in the DSC scan, as detailed in the Experimental Section): they may be, however, significantly increased by a well-adjusted annealing but without reaching the highest values typical of the free PTMO segment. For instance, in the case of the zwitterionomer Z67-S3-6, an annealing at room temperature for four weeks increases X_C from 0.28 to 0.31 and T_m from 22 to 45 °C.

All these features related to the influence of the PTMO segment length and of composition on crystallization of the copolymers are in good agreement with the general trends observed on segmented polyethers such as PTMO ionenes or poly(oxyethylene) polyurethanes[19] even if the chemical structure of the junctions may lead to significant differences: consider, for instance, the X_C value of about 0.3 for PTMO ionenes carrying a rather short PTMO segment, $M_n^0 \sim 1.8 \times 10^3$, and rigid bifunctional junctions of the bipyridinium halide type[15] ($W_B = 0.11-0.18$) while the zwitterionomers under study with similar PTMO segments are fully amorphous. The locking of the chain ends of the crystallizable PTMO segments in chemically different junctions which segregate in separate microdomains likely contributes to the strong decrease of the crystallinity degrees and melting temperatures.

Quantitative Analysis of the DSC Data in Terms of Biphasic Morphology. The analysis of the DSC data allows a quantitative description of the biphasic morphology in terms of relative importance of the soft and hard phases (weight fraction W^S and W^H, respectively) and of their internal composition (weight fraction W_i^j with i = A or B and j = S or H). The previously

Table 2. Compositional Data of the Amorphous Biphasic Copolymers As Derived from DSC Analysis (in All Cases $W_A^S = 1$)

copolymer	W_B	W^S	W_B^H	F_B^H	SR_S
Z22-E2-6	0.16	0.67	0.48	0.14	0.80
Z17-E2-3	0.18	0.67	0.54	0.18	0.81
Z20-E3-6	0.18	0.60	0.46	0.17	0.73
Z20-S3-6	0.16	0.65	0.47	0.14	0.78
Z17-S3−3	0.17	0.72	0.60	0.24	0.87
Z20-S4-6	0.17	0.67	0.52	0.16	0.80
I19-E-6	0.19	0.57	0.44	0.11	0.70
I19-S-6	0.18	0.67	0.55	0.17	0.82
Z19-E2	0.08	0.83	0.48	0.29	0.90
Z19-S3	0.07	0.86	0.53	0.35	0.92

noticed identity $T_g^S = T_g^{An}$ observed on all the segmented copolymers clearly shows that the soft matrix is essentially pure PTMO: $W_A^S = 1$. Straightforward calculations involving only the experimental heat capacity increment at T_g^S and a simple material balance lead to the following relations:

$$W^S = \Delta C_p^S/\Delta C_p^{An} \qquad W^H = 1 - W^S \tag{2}$$

$$W_B^H = W_B/(1 - W^S) \qquad W_A^H = 1 - W_B^H \tag{3}$$

$$SR_S = W^S/(1 - W_B) \tag{4}$$

where ΔC_p^{An} is the heat capacity increment at the glass transition of pure PTMO, $\Delta C_p^{An} = 0.72$ J·g^{-1}·K^{-1}.[20] The segregation rate SR_S[21,22] measures the fraction of nonpolar A units located in the nonpolar soft phase ($SR_S = 1$ corresponds to the ideal quantitative phase separation of the two components A and B). The accuracy of about ±5% on the ΔC_p^S values ($C_p^S \sim (0.3-0.5) \pm 0.02$ J·g^{-1}·K^{-1}) implies that W_B^H is not defined with an accuracy better than ±10%. The compositional data describing the two-phase morphology of all the amorphous segmented chains are given in Table 2.

It is highly tempting to compare the glass transition parameters of the hard phase (not involved in the previous calculations) with those of a copolymer or of a homogeneous blend of the same composition. This approach has been performed using the low molecular weight polyzwitterions PZ-S3-6 ($DP_w = 20$) and PZ-E2-6 ($DP_w = 22$) given below as model polymers for the S3-6 and E2-6 types of bifunctional junction.

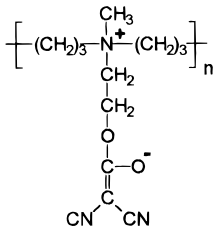

PZ-E2-6

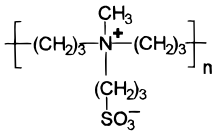

PZ-S3-6

The segmented zwitterionomer is thus considered as an $(A_xB_2)_n$ chain and the glass transition parameters of its hard phase are derived from its composition according to the Couchman equation[23] in its more general form for T_g^H and to a simple additivity rule for ΔC_p^H:

$$\ln T_g^H = \frac{W_A^H \Delta C_p^{An} \ln T_g^{An} + W_B^H \Delta C_p^{Bn} \ln T_g^{Bn}}{W_A^H \Delta C_p^{An} + W_B^H \Delta C_p^{Bn}} \tag{5}$$

$$\Delta C_p^{H*} = W_A^H \Delta C_p^{An} + W_B^H \Delta C_p^{Bn} \tag{6}$$

The comparison between the observed and calculated parameters of the high-temperature glass transition, given in Table 3, is, however, systematically biased by the choice of the glass transition parameters of the free PTMO chain for the calculation of the contribution of the TMO units rejected in the hard phase to its glass transition: these very short segments (see below), directly anchored to the zwitterionic aggregates, actually display strongly restricted mobility with respect to the free chain, as clearly shown by solid state ^{1}H NMR spectroscopy (see further in the text). Such a typical behavior has also been recently evidenced by high-resolution solid state ^{13}C-NMR spectroscopy on halatotelechelic polystyrenes where the sodium carboxylate multiplets are surrounded by a shell of strongly constrained styrene units located at the chain ends.[24] In the same way, the modeling of the contribution of the short difunctional junctions to the T_g^H through the T_g parameters of the polyzwitterions PZ-E2-6 and PZ-S3-6 is obviously oversimplified. Thus, the drastic underestimation of the calculated T_g^H values quoted in Table 3 are not surprising. On the other hand, the excellent agreement between the calculated ΔC_p^{H*} and the experimental and normalized $\Delta C_p^H/W_H$ values has likely no real physical meaning and may be incidental, favored by the rather narrow range of ΔC_p variations from PTMO to the model polyzwitterions. Finally, the previous comparison also implicitly implies that the two coexisting phases are independent while they are strongly interconnected by common chains crossing the interfaces and for such segregated structures the relaxations of the two phases are actually correlated.[25]

The structural parameters derived from the DSC analysis and detailed in Table 2 allow us to point out some common features of zwitterionomers and ionenes carrying a low molecular weight PTMO segment ($M_n^0 < 2.2 \times 10^3$) and various polar junctions.

(a) The pure PTMO soft matrix is the predominant phase and the segregation rates of the PTMO units in the matrix are high: $SR_S = 0.78 \pm 0.08$ and 0.90 for bifunctional and monofunctional junctions, respectively.

(b) The hard phase is not chemically homogeneous, and it is characterized by a molar content in TMO units much higher than in polar B units, even if it concentrates all the polar B junctions of the macromolecular chains. Thus, the values of the molar ratios $F_A^H/F_B^H = 5.9 \pm 1.4$ and 2.1 ± 0.03 for $f = 2$ and 1, respectively, show that on an average for a given copolymer chain, a zwitterionic or ionic site locks the two or three vicinal TMO units in the hard phase. This estimation may be critically discussed within the recent structural model developed by Eisenberg et al. for ionomers:[10] the apolar chain emerging from the polar multiplet is rigidified over a distance d similar to its persistence length q. For the PTMO chain, q is about 0.51 nm as derived according to Flory:[26] $C_\infty = (2q/l) - 1$, where the characteristic ratio C_∞ is 5.7[27] and the average bond length $l = 0.153$ nm. The upper and lower limits between the ends of a very short segment of 2 or 3 PTMO units may be estimated according to

$$d_{max} = L = N\sum n_i l_i \sin(\theta_i/2) \tag{7}$$

$$d_{min}^2 = (\bar{r}_0^2) = 2Lq - 2q^2[1 - \exp(-L/q)] \quad \text{(see ref 28)} \tag{8}$$

Table 3. Glass Transitions of the Model Polyzwitterions PZ-E2-6 and PZ-S3-6 and of the Hard Phase of Zwitterionomers Z22-E2-6 and Z22-S3-6

sample	T_g (°C)	ΔC_p (J·g^{-1}·K^{-1})	sample	T_g^H(exp) (°C)	T_g^H(calc) (°C)	$\Delta C_p^H/W_H$ (J·g^{-1}·K^{-1})	ΔC_p^{H*} (J·g^{-1}·K^{-1})
PZ-E2-6	110	0.34	Z22-E2-6	25	−33	0.54	0.52
PZ-S3-6	143	0.22	Z22-S3-6	38	−43	0.49	0.49

where L is the contour length of the segment in its fully extended conformation, N is the number of monomeric units, the parameters n_i, l_i, and θ_i being related to the number, the length, and the valence angle of the i bond. These two relations lead to the following d ranges:

$$2 \text{ TMO units} \qquad 0.9 \le d\,(\text{nm}) \le 1.2$$

$$3 \text{ TMO units} \qquad 1.2 \le d\,(\text{nm}) \le 1.8$$

These distances and more especially their upper limits corresponding to the most probable extended conformation[11,16,29] are actually higher than the persistence length, but they remain, however, of the same order of magnitude. Moreover, Eisenberg's concept may appear somewhat questionable since it involves the "static" parameter q for the interpretation of essentially dynamic phenomena.[11]

(c) The chemical structure of the polar junction between the PTMO blocks does not play a major role on the definition of the material morphology in terms of internal composition and relative importance of the coexisting phases: more specifically, there is no significant difference between zwitterionomers and ionenes at least at this level. However, the junction structure, together with the fraction of TMO units rejected in the hard phase W_A^H, determine the hard phase rigidity, as measured by its glass transition temperature. For a given junction R = $(CH_2)_6$, the decreasing order of efficiency of the zwitterions to promote high T_g values is

$$\text{S3} > \text{E2} > \text{S4} > \text{E3}$$

This order is parallel to that of the glass transition temperatures of homologous polyzwitterions in the (meth)acrylic series[30,31] and of the model homopolymers of the junctions (see Table 3). The value of the dipole moment of the zwitterionic function (μ = 24, 29.7, 25.9, and 30.8 D for S-3, S-4, E-2, and E-3, respectively[32]) does not appear as the unique parameter determining dipolar interactions and molecular motions, but its detailed chemical structure and steric factors are also likely pertinent factors. Our results do not allow a reliable analysis of the influence of the junction length x (R = $(CH_2)_x$). The increase from $x = 3$ to $x = 6$ has nearly no effect on T_g^H for the dicyanoethenolate zwitterionomers, while it significantly decreases T_g^H for the sulfonate ones. Finally, the ion-pair structure appears much less efficient than the homologous zwitterionic function for promoting a strong cohesion of the hard phase.

Comparison of the results with literature data on similar biphasic systems points out (a) a definite analogy with some segmented PTMO of the ionene[13−15] or polyurethane[21] type which, however, display significantly lower segregation rate SR_S in the latter case ($SR_S \sim 0.6$) and (b) very typical differences with *n*-butyl acrylate zwitterionomers of the ammoniopropanesulfonate (ABu-S3)[1] or (ammonioethoxy)dicyanoethenolate (ABu-E2)[5] type and of the same molar composition, illustrated below:

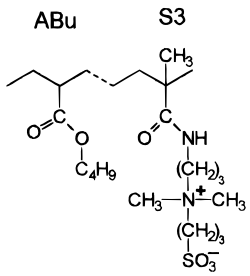

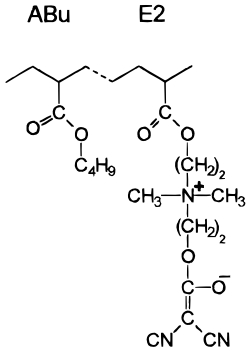

For these statistical copolymers (Bernoullian distribution in the case of the ABu-E2 copolymer[33]), two features may be stressed: (i) The chains of lower zwitterion content ($F_B < 0.04$ for ABu-S3, $F_B < 0.06$ for ABu-E2) lead to monophasic materials, in sharp contrast with segmented PTMO zwitterionomers of similar composition Z19-E2 and Z19-S3 ($F_B = 0.04$). (ii) A weak but still significant fraction of the dipolar units is always rejected in the matrix, more especially for the copolymer ABu-E2: compare, for instance, $W_B^S = 0.11$ for a ABu-E2 sample of $F_B = 0.09$ ($W_B = 0.18$) with $W_B^S = 0$ for segmented zwitterionomers of similar composition Z17-E2-3 and Z17-S3-3, $F_B = 0.09$ ($W_B = 0.18$ and 0.17, respectively). The higher mobility and the weaker polarity of the PTMO matrix ($T_g = -77$ °C, Hildebrand solubility parameter $\delta_H = 17.4$ (J·mol^{-1})$^{0.5}$,[34] dipole moment $(\mu^2/N)^{0.5} = 1.1$ D[35]), with respect to those of poly(butylmethacrylate) ($T_g = -46$ °C, $\delta_H = 17.4$ (J·mol^{-1})$^{0.5}$,[36] $(\mu^2/N)^{0.5} = 1.52$ D[37]), may contribute to the observed better phase separation, but the regular distribution of the dipolar units typical of the segmented chain is very likely the major factor of such an improvement.

Structural Analysis through Solid State ^{1}H-NMR Spectroscopy. The study of chain dynamics by wideline ^{1}H-NMR spectroscopy has been performed on five representative copolymers: the two zwitterionomers Z20-E2-6 and Z22-S3-6 and their homologous ionenes I19-E-6 and I19-S-6 on one hand, allowing comparison between amorphous segmented copolymers carrying bifunctional junctions of various structures, and the zwitterionomer Z52-E2-6 on the other hand, as a representative semicrystalline copolymer.

^{1}H Dipolar Line Shape Analysis. It was performed over a broad temperature range from −80 to +160 °C: the free induction decays (FID's) of the copolymers were decomposed into components of exponential or Gaussian shape of strongly different time constants corresponding to coexisting phases of different mobilities. A representative example of the data analysis is given in Figure 3. For a given copolymer at a given temperature, extrapolation of the data to the FID time origin yields directly their relative importance. This procedure allows the derivation of a structural map giving the sample composition in terms of fractions (measured in H nuclei) of a rigid (Gaussian component of lower T_2, $T_2 \sim 10$ μs), an intermediate (Gaussian component of higher T_2, $T_2 \sim 30$ μs), and a mobile (exponential component of $T_2 > 50$ μs) phase at any temperature.

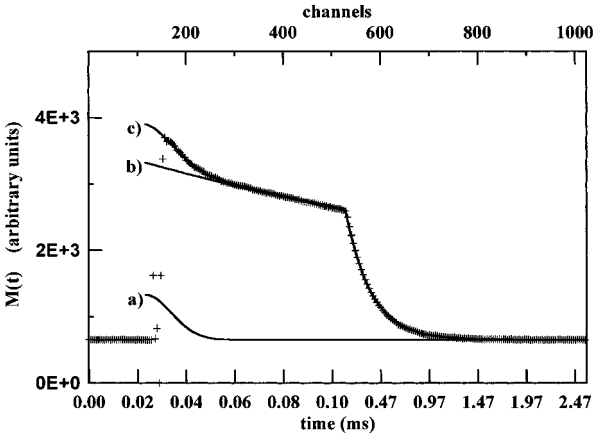

Figure 3. ^{1}H-FID of the zwitterionomer Z22-E2-6 at 30 °C. The signal (+) is recorded with a 0.2 μs dwell during 528 channels, then with a 20 μs dwell during 496 channels. The sum (c) of an exponential (b) and a Gaussian (a) is fitted (five parameters) to the original signal: $M(t) = 2698 \exp(-t/263\ \mu s) + 532 \exp[-0.5(t/12\ \mu s)^2]$. The rigid (Gaussian) and mobile (exponential) fractions are 0.17 and 0.83, respectively. For the Gaussian component, $M_2^R = 9.7$ G^2, the overall M_2 being 1.65 G^2.

The structural maps of the amorphous copolymers given in Figure 4 allow us to separate two temperature ranges.

(a) At low temperatures, $T < 20$ °C, the very strong increase of the mobile fraction in the materials between −70 and −30 °C is essentially related to the glass transition of the flexible PTMO segments.

(b) At high temperatures, $T > 20$ °C, the intermediate fraction can no longer be readily identified and the rigid phases still persist at very high temperatures, more than 60 deg above their glass transitions, as previously determined in DSC measurements. The decreasing order of their thermal stability is given below with the temperature when the whole material reaches the liquid state:

Z20-S3-6 (160 °C) > Z22-E2-6 (120 °C) > I19-E-6 (100 °C) ~ I19-S-6 (100 °C)

This sequence is in good agreement with that previously observed through DSC.

The semicrystalline zwitterionomer Z52-E2-6 is essentially characterized by two specific features, as shown in Figure 5.

(a) The very strong decrease of its rigid fraction between 10 and 20 °C is directly correlated with the melting of partly crystallized PTMO segments, as already noticed in DSC: T_m(DSC) = 19 °C, T_m(NMR) = 15 °C. If the contribution of the amorphous fraction is neglected in a first approach, the rapid drop of the rigid fraction may be ascribed only to the H nuclei of the crystalline PTMO segments: the crystallinity degree thus calculated is $X_C = 0.29$, and this overestimated value is consistent with the DSC one, $X_C = 0.22$, taking into account the previous assumption and the different thermal histories of the copolymer in the two types of measurements.

(b) After the PTMO melting, a rigid phase is still observed up to 120 °C (Gaussian component with a characteristic second moment M_2^R of at least 8 G^2; see further in the text), while DSC measurements were unable to identify any hard phase with a characteristic

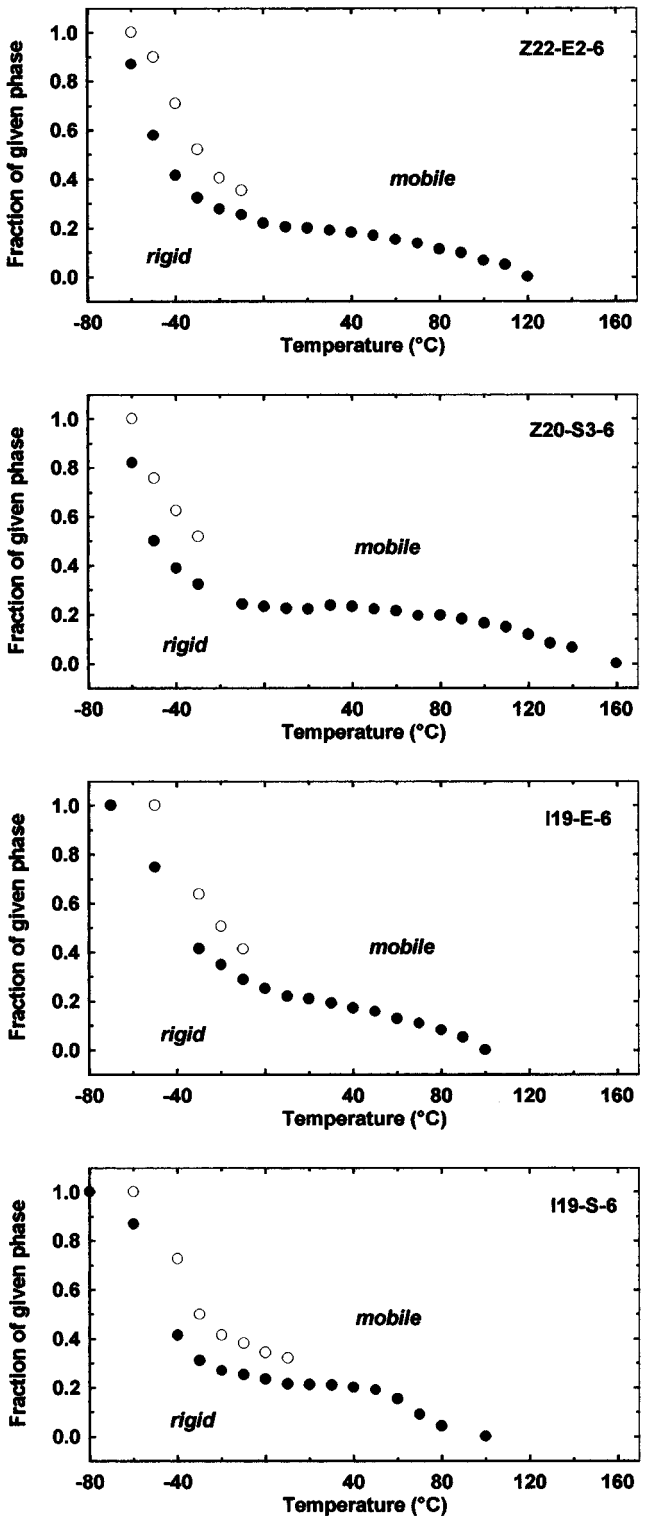

Figure 4. Line shape analysis for four homologous amorphous zwitterionomers and ionenes: temperature dependence of the ^{1}H fraction of the rigid component (●) and of the ^{1}H-cumulated fractions of the rigid + intermediate components (○).

glass transition. Its weakness fraction merely reflects the low zwitterionic content of this copolymer (Φ_B = 0.04).

$T_1\rho$ Analysis. In order to have a better morphological description of the amorphous copolymers well above the glass transition of the PTMO matrix, the $T_1\rho$ relaxation curves related to faster molecular motions (10−100 kHz instead of 1−10 kHz for line shape analysis) were analyzed between 20 and 160 °C. De-

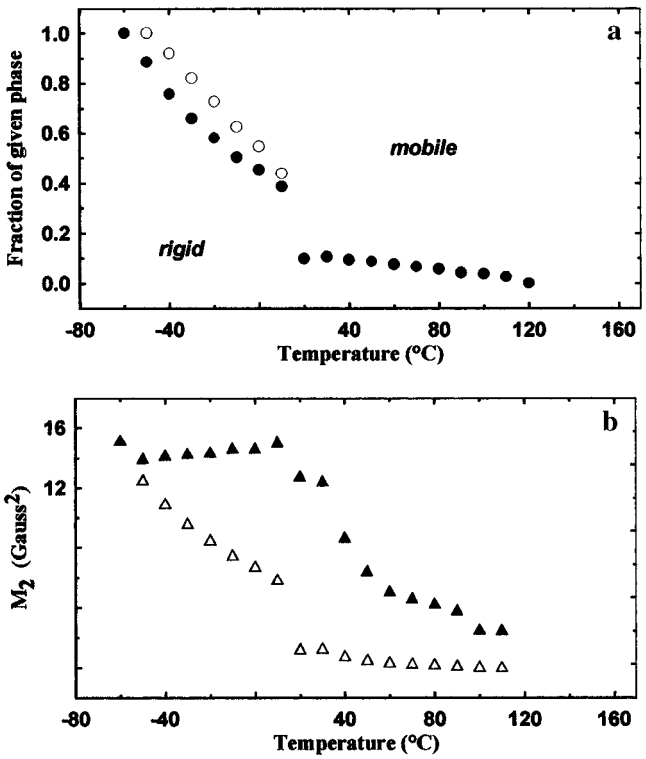

Figure 5. Line shape analysis for the semicrystalline zwitterionomer Z52-E2-6: (a) temperature dependence of the ^{1}H fraction of the rigid component (▲) and of the ^{1}H-cumulated fractions of the rigid + intermediate components (△). (b) Temperature dependence of the second moment of the rigid component (▲) and of the whole band (△).

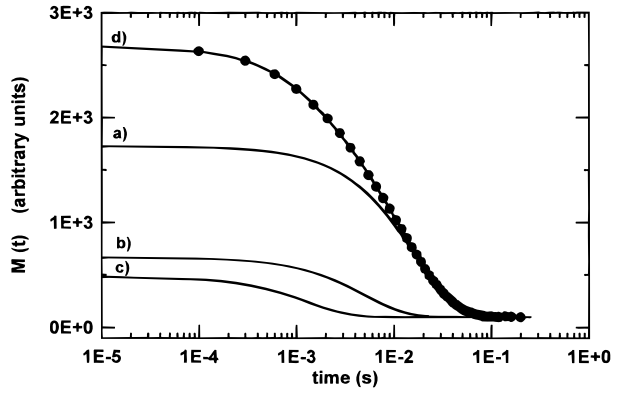

Figure 6. $T_1\rho$ analysis for the zwitterionomer Z22-E2-6 at 30 °C. The overall decay is sampled on 50 points (●). The sum of three exponentials *a*, *b*, *c* (decreasing $T_1\rho$ values) is fitted (seven parameters) to the original decay: $M(t) = 1626 \exp(-t/16.4\ \text{ms}) + 568 \exp(-t/5.0\ \text{ms}) + 387 \exp(-t/1.3\ \text{ms})$. The mobile (a), intermediate (b), and rigid (c) fractions are 0.63, 0.22, and 0.15, respectively.

convolution in discrete components, illustrated in Figure 6, allows us to separate three exponentials characterized by strongly different relaxation times $T_1\rho$ (about one decade over the whole temperature range): they may be unambiguously ascribed to a rigid ($T_1\rho \sim 0.5-4$ ms), intermediate ($T_1\rho \sim 4-9$ ms), and mobile ($T_1\rho \sim 15-40$ ms) phase, respectively, according to their variations with temperature and along the FID. The structural maps derived from such an analysis are given in Figure 7.

Second Moments. Finally, the variations of the second moments of the NMR bands with temperature are illustrated in Figure 8: the second moment related to the rigid fraction M_2^R and the overall second moment

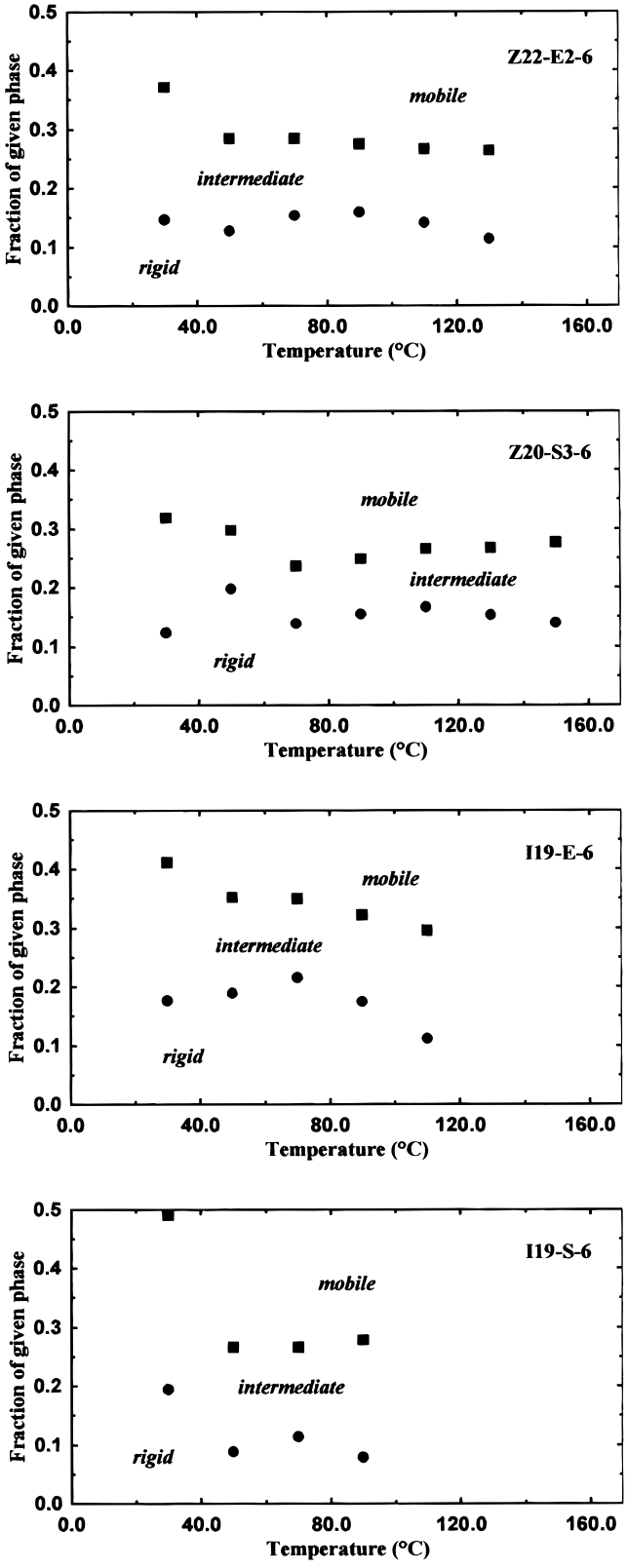

Figure 7. $T_1\rho$ analysis for four homologous amorphous zwitterionomers and ionenes: temperature dependence of the ^{1}H fraction of the rigid component (●) and of the ^{1}H cumulated fractions of the rigid + intermediate components (■) (same copolymers as in Figure 4).

of the whole resonance band M_2 recalculated from the contributions of its components according to $M_2 = \sum_i f_i M_{2i}$. The M_2 variations are dominated by the major contribution of predominant PTMO matrix, and they essentially reflect its glass transition (strong M_2 decrease between −60 and −40 °C). The variations of the

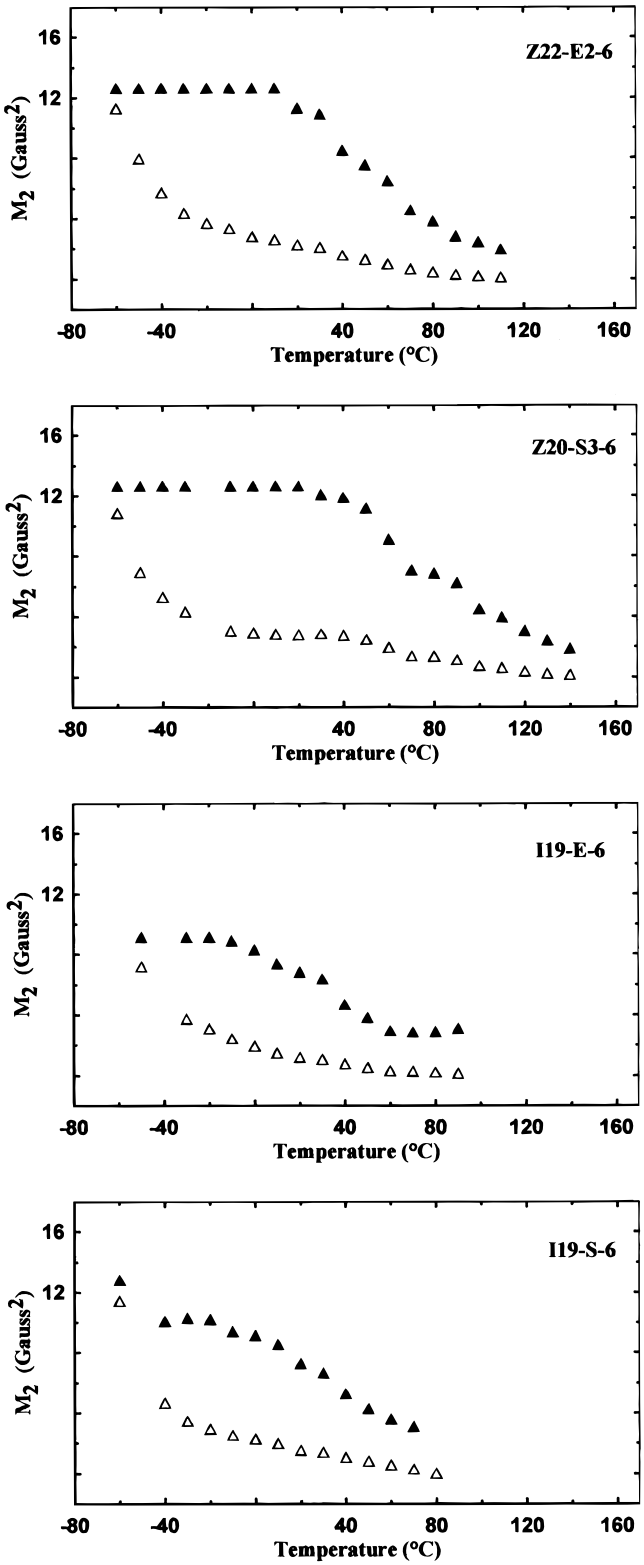

Figure 8. Temperature dependence of the second moments related to the rigid fraction (▲) or to the whole copolymer (△) for four homologous zwitterionomers and ionenes (same copolymers as in Figure 4).

second moment M_2^R clearly show the persistence of a rigid phase well above the glass transition of the matrix. In the case of the semicrystalline zwitterionomer Z52-E2-6, the melting of the crystallized PTMO segments is well identified by the very sharp decrease of M_2 between 10 and 20 °C and the persistence of a rigid phase at higher temperatures is well ascertained by the still high M_2^R values (see Figure 5).

Table 4. Comparison between the Compositional Data (Normalized ^{1}H Fractions Φ_i) of Representative Biphasic Copolymers As Derived from DSC and from ^{1}H Solid State NMR Analysis (Line Shape and $T_1\rho$ Analysis)

		DSC			NMR				
copolymer	Φ_B	T_g^S (°C)	T_g^H (°C)	Φ_H	T_g^S (°C)	T_g^H (°C)	Φ_R	Φ_R^*	$\Phi_R^* + \Phi_I^*$
Z22-E2-6	0.10	−77	25	0.28	-50	60	0.20	0.14	0.28
Z20-S3-6	0.12	−77	38	0.31	-50	70	0.24	0.15	0.27
I19-E-6	0.14	−75	6	0.42	−45	40	0.18	0.17	0.35
I19-S-6	0.15	−77	−4	0.31	−50	40	0.22	0.10	0.27
Z52-E2-6[a]	0.04	−78					0.10		

[a] Semicrystalline zwitterionomer where the hard phase cannot be quantified through DSC.

Comparison between the Structural Analysis Performed through DSC and Solid State ^{1}H-NMR Spectroscopy for the Amorphous Zwitterionomers and Ionenes. It is based on the following assumptions: (i) the glass transition temperature is conventionally measured at the half-value of the M_2 plateau; (ii) characteristic values of the fraction of rigid phases Φ_R oand Φ_R^* (line shape or $T_1\rho$ analysis) and of the intermediate phase Φ_I^* ($T_1\rho$ analysis) are determined within a rather narrow temperature range between the two glass transitions where their fluctuations are safely negligible (about 0−40 °C for line shape and 40−100 °C for $T_1\rho$ analysis). The experimental results given in Table 4 point out some interesting features.

(a) The NMR glass transition temperatures are systematically higher than the corresponding DSC ones ($\Delta T_g^S \sim 25$ °C, $\Delta T_g^H \sim 35$ °C), but this apparent discrepancy merely arises from the difference between the two techniques with respect to the measurement frequency.

(b) The fraction of hard phase identified through DSC is systematically higher than the fraction of rigid phase derived from the line shape analysis: this type of NMR measurements, which does not allow us to quantify the intermediate phase (see above), may likely result in an overestimation of the mobile phase.

(c) There is a very good agreement between the fraction of hard phase and the overall fraction of rigid and intermediate phases derived from the $T_1\rho$ analysis, probably because the higher $T_1\rho$ contrast allows a better deconvolution, compared to line shape analysis: $\Phi_H = (1.1 \pm 0.1)(\Phi_R^* + \Phi_I^*)$. However the fractions of rigid phase appear generally slightly higher than the fraction of polar junction Φ_B in the segmented copolymers.

Thus the structural data derived from DSC and solid state NMR spectroscopy can be considered very self-consistent, and a better quantitative agreement cannot be reasonably expected since the two techniques test chain dynamics in the materials at different scales and frequencies. A conclusion of major interest is the unambiguous NMR identification of the intermediate phase through $T_1\rho$ analysis: it may be at least qualitatively correlated with the few TMO units of restricted mobility directly anchored to the rigid polar multiplets which are directly involved in the cluster formation, as defined in the multiplet−cluster concept.[10]

Conclusion

According to the previous structural analysis relying on two independent techniques free from any strong assumption, all the PTMO segmented copolymers display a typical biphasic morphology characterized by three common features:

•the presence of a highly predominant mobile matrix (about 65 to 85% of the total material) of pure PTMO (T_g^S(DSC) = −77 °C)

•the presence of a hard phase (T_g^H(DSC) ∼ −6 to +38 °C) where all the polar junctions are concentrated and where every polar unit locks and rigidifies about two or three vicinal TMO monomeric units

•the very high thermal stability of the polar aggregates which still persist at temperatures much higher than the glass transition of the hard phase

Obviously, this two-phase morphology is in good agreement with the multiplet−cluster concept recently revisited by Eisenberg et al.[10]

At this stage of the structural analysis, the chemical nature of the polar junction does not play a major role in terms of internal composition and relative importance of the coexisting phases. It is, however, of definite importance for promoting higher rigidity and thermal stability of the multiplets and clusters: the zwitterionic structure is more efficient than the homologous ion-pair structure and, among the quaternary ammonio zwitterions, the propanesulfonate is more efficient than the ethoxydicyanoethenolate. On the other hand, always at this stage of the structural analysis, the main difference between segmented and statistical zwitterionomers lies in an earlier (lower polar content) and by far better phase separation in the former case.

The dimensionality and size of the rigid multiplets, as studied by Goldman−Shen spin diffusion, and the major role of the chain topology and of the chemical structure of the polar junctions in the development of long range order in these copolymers, as studied by small-angle X-ray and neutron scattering, will be discussed in forthcoming papers. It will be shown that only bifunctional zwitterionomers actually display long range order, with a typical structural transition from lamellar to hexagonal morphology when their zwitterionic content is decreased.[16]

References and Notes

(1) Ehrmann, M.; Mathis, A.; Meurer, B.; Scheer, M.; Galin, J. C. *Macromolecules* **1992**, *25*, 2253.
(2) Ehrmann, M.; Galin, J. C.; Meurer, B. *Macromolecules* **1993**, *26*, 988.
(3) Ehrmann, M.; Muller, R.; Galin, J. C.; Bazuin, C. G. *Macromolecules* **1993**, *26*, 4910.
(4) Galin, M.; Mathis, A.; Galin, J. C. *Macromolecules* **1993**, *26*, 4919.
(5) Gingreau, C. Thesis, Strasbourg, December 1993.
(6) Eisenberg, A.; King, M. *Ion Containing Polymers*; Academic Press: New York, 1977.
(7) MacKnight, W. J.; Earnest, T. R. *J. Polym. Sci., Macromol. Rev.* **1981**, *16*, 41.
(8) Mauritz, K. A. *J. Macromol. Sci., Rev. Macromol. Chem. Phys. C* **1988**, *28*, 65.
(9) Fitzgerald, J. J.; Weiss, R. A. *J. Macromol. Sci., Rev. Macromol. Chem. Phys. C* **1988**, *28*, 99.
(10) Eisenberg, A.; Hird, B.; Moore, B. *Macromolecules* **1990**, *23*, 4098.
(11) Nyrkova, I. A.; Khokhlov, A. R.; Doi, M. *Macromolecules* **1993**, *26*, 3601.
(12) Grassl, B.; Galin, J. C. *Macromolecules* **1995**, *28*, 7036.
(13) Feng, D.; Venkateshwaran, L. N.; Wilkes, G. L.; Leir, C. M.; Stark, J. E. *J. Appl. Polym. Sci.* **1989**, *38*, 1549.
(14) Feng, D.; Wilkes, G. L.; Lee, B.; McGrath, J. E. *Polymer* **1992**, *33*, 526.
(15) Hashimoto, T.; Sakurai, S.; Morimoto, M.; Nomura, S.; Kohjiya, S.; Kodaira, T. *Polymer* **1994**, *35*, 2672.
(16) Grassl, B. Thesis, Strasbourg, November 1995.
(17) McBrierty, V. J.; Packer, K. J. *Nuclear Magnetic Resonance in Solid Polymers*; Cambridge University Press: Cambridge, U.K., 1993; p 90 (FID) and p 98 ($T_1\rho$).
(18) Kretz, M.; Meurer, B.; Lotz, B.; Weill, G. *J. Polym. Sci., Polym. Phys. Ed.* **1988**, *23*, 663.
(19) Galin, J. C.; Spegt, P.; Suzuki, S.; Skoulios, A. *Makromol. Chem.* **1974**, *175*, 991.
(20) Suzuki, M.; Wunderlich, B. *J. Polym. Sci., Polym. Phys. Ed.* **1985**, *23*, 1671.
(21) Camberlin, Y.; Pascault, J. P. *J. Polym. Sci., Polym. Chem. Ed.* **1983**, *21*, 415.
(22) Wagener, K. B.; Matayabas, J. R. *Macromolecules* **1991**, *24*, 618.
(23) Couchman, P. R. *Macromolecules* **1983**, *16*, 1924.
(24) Van Hoorne, P.; Jerome, R.; Teyssie, P.; Laupretre, F. *Macromolecules* **1994**, *27*, 2548.
(25) Leibler, L.; Rubinstein, M.; Colby, R. H. *Macromolecules* **1991**, *24*, 4701.
(26) Flory, P. J. *Statistical Mechanics of Chain Molecules*; Interscience: New York, 1969; p 111.
(27) Braudrup, J.; Immergut, E. H. *Polymer Handbook*, 2nd ed.; John Wiley & Sons, New York, 1975.
(28) Benoit, H.; Doty, P. *J. Phys. Chem.* **1965**, *57*, 958.
(29) The zwitterionomers of high zwitterionic content show a lamellar morphology where the PTMO chain is actually extended by about 50% with respect to its unperturbed end to end distance.[16]
(30) Galin, J. C.; Galin, M. *J. Polym. Sci., Polym. Phys. Ed.* **1992**, *30*, 1103.
(31) Galin, J. C.; Galin, M. *J. Polym. Sci., Polym. Phys. Ed.* **1995**, *33*, 2033.
(32) Galin, M.; Chapoton, A.; Galin, J. C. *J. Chem. Soc., Perkin Trans. 2* **1993**, 545.
(33) Gingreau, C.; Galin, J. C. *Polymer* **1994**, *35*, 4669.
(34) Dreyfuss, P. *Poly(tetrahydrofuran)*; Gordon & Breach Science Publishers: New York, 1982; p 153.
(35) Wetton, R. E.; Williams, G. *Trans. Faraday Soc.* **1965**, *61*, 2132.
(36) Mangaraj, D.; Patra, S.; Rath, S. B. *Makromol. Chem.* **1963**, *67*, 84.
(37) Hedrig, P. *Dielectric Spectroscopy of Polymers*; A. Hilger, Ltd.: Bristol, U.K., 1977; p 26.

MA960643S